

The Potential of the Display with Path Motion Prediction and Preview of the Planned Trajectory

A. Efremov, M. Tiaglik, I. Irgaleev

Abstract A general approach to selecting an algorithm for the predictive display and for optimizing the prediction time is proposed. Two algorithms were developed. One for an aircraft landing task and the other for a spacecraft docking task. The potential to compensate the time delay for both vehicles is demonstrated. The algorithms also demonstrated the potential to suppress the actuator rate limit effect. The integration of the predictive display with preview information about the planned trajectory is investigated in the paper.

1 Introduction

The precise path control task is one of the most difficult manual control tasks for aeronautical and space vehicles because of the high order pole at the origin of the controlled element dynamics. For example the transfer function between the elevator (thruster) and altitude of the aircraft in a landing task, the spacecraft in docking with the International Space Station (ISS), when the pilot (astronaut) tracks the altitude, has the second order pole at the origin. It requires considerable pilot lead compensation which decreases the accuracy.

A. Efremov
Moscow Aviation Institute, Moscow, 125993, Volokolamskoe shosse, 4,
e-mail: pvl@mai.ru

M. Tiaglik
Moscow Aviation Institute, Moscow, 125993, Volokolamskoe shosse, 4,
e-mail: pvl@mai.ru

I. Irgaleev
Moscow Aviation Institute, Moscow, 125993, Volokolamskoe shosse, 4,
e-mail: pvl@mai.ru

The modern highly augmented flight control system allows to transform the aircraft dynamics considerably and to provide the necessary flying qualities [1-3]. Simultaneously with such potentialities, aircraft with such control systems is characterized by a number of dynamic peculiarities. One of them is the additional phase delay caused by the digital realization of control laws, different filters and prefilters installed in the flight control system to suppress the rate limit effects of the actuator. The dynamic effect of all these elements is equivalent to the time delay whose value reaches 0.15 - 0.3 sec for highly augmented vehicles. This peculiarity causes the deterioration of the pilot-vehicle system dynamic characteristics and appearance of the so-called pilot-induced oscillations (PIO) (Category 1) [4]. The negative side effects of the pilot-aircraft system characteristics can be suppressed by the adaptive prefilters [5] or an active inceptor with variable spring stiffness [6]. Such means allow to eliminate the PIO events but they are effective in cases when the time delay does not exceed 0.3 - 0.4 sec [5].

The teleoperator mode used for spacecraft docking with the ISS and the UAV control implemented via satellite is accompanied by a higher time delay (up to 1 - 1.2 sec) [7]. Manual control is much more complicated in these cases which requires the special means. This provides a considerable decrease of pilot workload and improvement of accuracy. The Lunar rover teleoperator control is characterized by a considerably higher time delay (close to 4 sec). Such delays lead to the discretization of the pilot's commands, the so-called "stop and go" type of piloting strategy which decreases the rover's opportunities to explore the planet. The alternative solution is the automatic control which is used widely now.

Another peculiarity of highly augmented aircraft is the actuator rate limit. It is one of the main sources of the pilot-induced oscillation events and requires the installation of special means (for example prefilters) to suppress it. This solution is accompanied by side effects because of an increase in the time delay in the controlled element dynamics.

The problem discussed in the paper is dedicated to the search for a way to realize manual control for such vehicles by the compensating the time delay in their response and actuator rate limit effects by use of the predictive display.

In practically in all applied manual tasks the pilot-aircraft system is considered as a compensatory system where pilot perceives and reacts to the error between the input and output signal. The case when the pilot has the ability to perceive the future input signal in addition to the current one transforms the system from compensatory to preview. Such type of display investigated in [8] for simple dynamic configuration demonstrated high potential to improve the accuracy. The potentialities of the planned trajectory preview and optimization of preview time are discussed below.

2 The General Principles of Predictive Display Design

The usefulness of the predictive display in aircraft landing was shown in [9, 10]. In [10] the predictive display was proposed for the landing on a carrier and refueling task. It displays a 3D corridor in which the aircraft has to move. This display also demonstrates the surface moving inside the corridor with the aircraft

velocity V and the predictive angle $\varepsilon_{pr} = \gamma_{pr} + \frac{\Delta H}{L_{pr}}$ (here L_{pr} is the distance between the pilot and the moving surface, $\gamma_{pr} = \gamma + \dot{\gamma} \frac{T_{pr}}{2}$ - the predictive path angle, $T_{pr} = \frac{L_{pr}}{V}$ - the prediction time, ΔH - the change of aircraft altitude).

Thus the equation for the predictive angle ε_{pr} is:

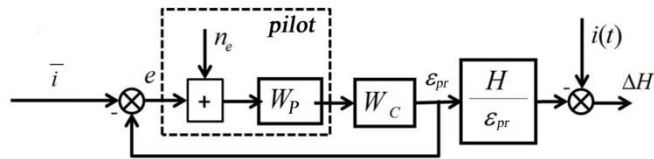
$$\varepsilon_{pr} = \frac{\Delta H}{L_{pr}} + \gamma + \dot{\gamma} \frac{T_{pr}}{2} \quad (1).$$

The pilot's perception of the angle ε_{pr} allows him to evaluate the aircraft position at the moment $(t + T_{pr})$. In the case where the pilot closes the loop with ε_{pr} as the output signal, the controlled element dynamics transform from $W_c = \frac{H(j\omega)}{\delta_e(j\omega)}$ to $\frac{\varepsilon_{pr}(j\omega)}{\delta_e(j\omega)}$. It provides slope of amplitude frequency response characteristics in a crossover frequency band close to -20 dB/dec which improves the accuracy and decreases the pilot workload. A technique for synthesizing the predictive law for a case in which time delay was absent in the vehicle dynamic response was considered in [10].

Briefly the technique consists of the following:

1. Consideration of pilot-vehicle systems (fig.1)

Fig. 1 Pilot-vehicle system



Here W_p is the pilot describing function and n_e - the pilot's remnant. The elements of the system \bar{i} , W_c , $\frac{H}{\varepsilon_{pr}}$ depend on the T_{pr} (or L_{pr}). In particular

for aircraft landing: $\bar{i} = \frac{i(t+T_{pr})}{L_{pr}}$; $\frac{H}{\varepsilon_{pr}} = \frac{2V}{T_{pr}^2 s^2 + 2s + \frac{2}{T_{pr}}}$ and the con-

trolled element dynamics

$$W_c = \frac{K_c (T_{pr}^2 s^2 + 2s + \frac{2}{T_{pr}})}{2s^2 (s^2 + 2\xi_{sp} \omega_{sp} s + \omega_{sp}^2)} \quad (2)$$

where ξ_{sp} is the damping of short period motion, ω_{sp} is the frequency of short period motion, V is the aircraft velocity.

The increase in the prediction time T_{pr} leads to the improvement of accuracy (decrease in the variance of error σ_e^2) because of the reduction in the phase frequency response of the controlled element dynamics. It also influences the transfer function $\frac{H(s)}{\varepsilon_{pr}(s)}$. For T_{pr} close to zero, the order pole at the origin of this

function $\frac{H(s)}{\varepsilon_{pr}(s)}$ is equal to zero. According to [10] such type of coupling does

not require the closure of the outer loop. At the same time when $T_{pr} \gg 1$ it is close to the second pole order at the origin which requires closing the outer loop with considerable pilot lead compensation in it. The increase of T_{pr} decreases the amplitude of input signal $\bar{i}(t)$ and as a consequence the perceived error signal $e(t)$. It causes the increase of influence of the perceptual threshold and pilot remnant [10].

As the prediction time T_{pr} influences the considered elements in the opposite way its optimization has to be carried out.

2. The selection of the prediction time T_{pr} is carried out by the minimization of the variance of altitude error in mathematical modeling of the pilot-vehicle system and by the following verification of results in ground based simulation.

For the mathematical modeling a modified pilot structural model was developed in [10]. The optimization of T_{pr} is carried out in three stages. In the first stage the parameters of the pilot structural model and the variance of predictive angle $\sigma_{\varepsilon_{pr}}^2$ corresponding to them are selected. The structural model includes the model of the remnant spectral density $S_{n_e n_e}(\omega)$ and the pilot describing function $W_p(j\omega)$. In the second stage the time responses of the pilot-vehicle system and the variance of altitude error $\sigma_{\Delta H}^2$ are calculated by the Simulink package for each set of pilot parameters obtained in the first stage. Finally the

dependence $\sigma_{\Delta H}^2 = f(T_{pr})$ is defined. This allows to get the optimum value of T_{pr} . All these procedures are considered in [10] in detail.

It is necessary to note that the use of the equation (1) as the predictive angle for the spacecraft display used for docking task has its shortcoming. It is seen from the analysis of the control element dynamic frequency response characteristic $W_c = \frac{\varepsilon_{pr}(j\omega)}{\delta_e(j\omega)}$ shown in fig. 2 (solid line). The slope of its amplitude re-

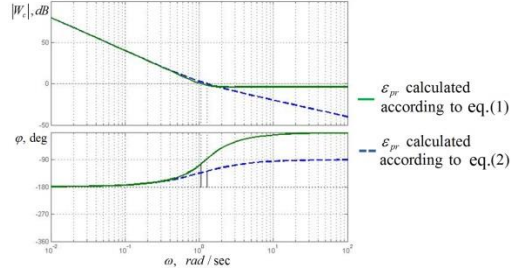
sponse characteristics in the crossover and high frequency bands ($\frac{d20\lg|W_c|}{d\lg|\omega|}$)

is equal to 0. It means that the provision of acceptable open loop frequency response characteristics in these bands ($\frac{d20\lg|W_{OL}|}{d\lg|\omega|}$) require the pilot's lag compensation which increases the pilot workload.

In case when the predictive angle will be defined by the equation:

$$\varepsilon_{pr} = \frac{\Delta H}{L_{pr}} + \gamma(s) \quad (3)$$

Fig. 2 Controlled element dynamics of a space vehicle in a docking task



the slope of the amplitude frequency response characteristics of $W_c(j\omega)$ is equal to -20 dB/dec in the crossover frequency range (dotted line fig.2) which does not require pilot's compensation in this frequency range.

3 Application of the General Technique to Some Manual Control Tasks

In case of a nonzero time delay in transmitting the command signal from the pilot to the control surface (thruster) the flying qualities deteriorate considerably. The increased phase delay requires pilot lead compensation. It causes the deterioration of the pilot-vehicle system characteristics.

For the suppression of the time delay effect, the predictive path angle γ_{pr}^* in equation 1 or equation 2 by on-board computer was calculated.

For a docking task such summand is the calculated path angle γ^* and the predictive angle is

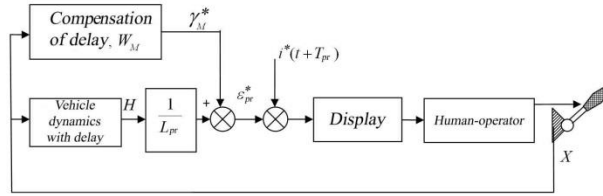
$$\varepsilon_{pr} = \frac{\Delta H \cdot e^{-s\tau}}{L_{pr}} + \gamma^*, \quad (4)$$

for an aircraft in a landing task γ^* is $\gamma^* \frac{T_{pr}}{2}$ and

$$\varepsilon_{pr} = \left(\frac{\Delta H}{L_{pr}} + \gamma \right) e^{-s\tau} + \dot{\gamma}^* \frac{T_{pr}}{2}. \quad (5)$$

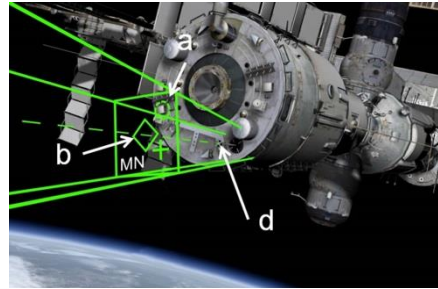
2.1 The Suppression of the Time Delay in a Docking Task with the ISS

Fig. 3 Pilot-aircraft system with compensation of the time delay



The principle of compensating the time delay realizing the equation (4) is given in fig.3. The display is shown in fig. 4 for a docking task. Here the 3D corridor is the planned trajectory. Inside it the surface MN moves with the velocity of the vehicle. The center of the rhombus “b” located on the surface MN lies on the line passing through the target located on the ISS (d). In the experiment the predictive angle ε_{pr} (the angle between the centerline of the corridor and calculated projection of velocity) was displayed as the signal “a”. The distance between the spacecraft and the surface MN is equal to $L_{pr} = VT_{pr}$.

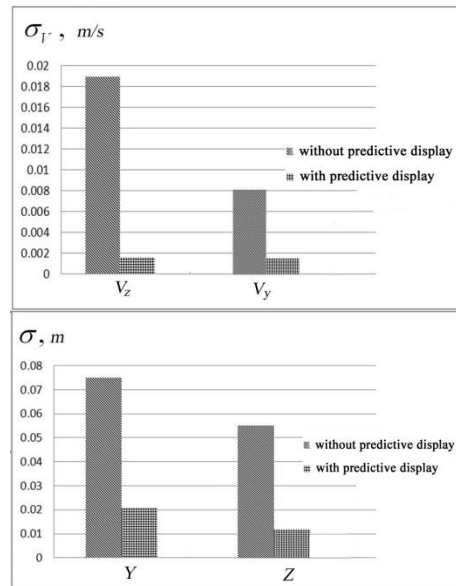
Fig. 4 The predictive display



In case of teleoperator control of the spacecraft when docking with the ISS, the controlled element dynamics transfer function is $W_c = \frac{K_c(T_{pr}s + e^{-\tau s})}{T_{pr}s^2(Ts + 1)}$ (T is the equivalent time constant of the thruster dynamics).

The optimization of T_{pr} was carried out according to the technique considered above which allowed to get its optimum value equal to 16 - 18 sec. In the experimental investigations the pilot's task was to combine three points: the center of 3D corridor (point "b"), the projection of the predictive path angle (point "a") and the target "d". The results of ground-based simulation demonstrated the high potential of the predictive display to decrease the mean square errors of the velocities (V_y, V_z) and the linear coordinates Z, Y considerably (see fig.5).

Fig. 5 Accuracy of the glide slope tracking



2.2 The Suppression of the Time Delay in an Aircraft Landing Task

The effect of the time delay suppression was investigated for two dynamic configurations characterized by different time delays ($\tau = 0, \tau = 0.18$ sec). Their frequency response characteristics are given in fig.6.

The usage of the calculated path rate $\dot{\gamma}^*$ instead of a measured one allowed to suppress the effect of time delay (see fig. 7). The frequency response characteristics of the controlled element dynamics are practically the same as those for the case of zero time delay.

Fig. 6 Influence of the time delay

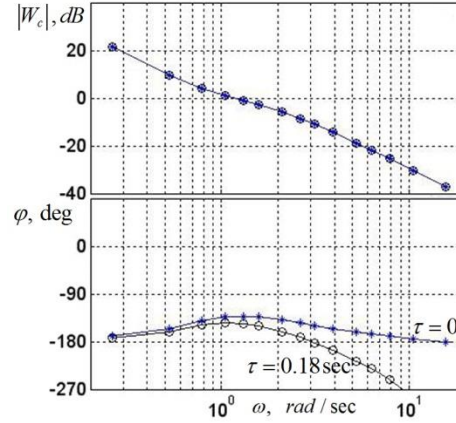
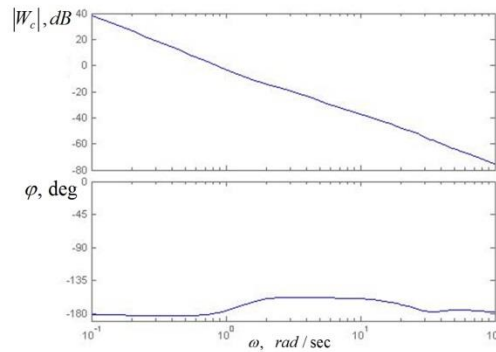


Fig. 7 Controlled element dynamics with compensation of time delay



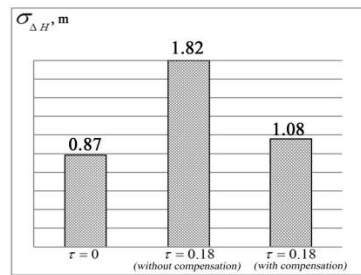
The mathematical modeling of the pilot-aircraft system was carried out according to the procedure given in [10]. This allowed to get the optimum value T_{pr} . In particular it was obtained that $T_{pr_{opt}} = 1.4 \text{ sec}$ which is higher than the value $T_{pr} = 0.9 \text{ sec}$ obtained for the case when time delay is zero. The results of the mathematical modeling were verified in a ground based simulation. The simulator was equipped with a stereoscopic computer-generated visual system with a wide angle of view. The piloting task was to align the projection of the predictive angle ε_{pr} on the moving surface with its center. The image predictive display was projected on the image of the surrounding space (fig. 8). Three operators participated in the experiments. One of them has a pilot's license and two have a practice of flying as the co-pilot and a rich experience on flying on the simulators. At least six experiments were carried out for each dynamic configuration. In the experiments on the simulators the harmonic disturbance with a frequency equal to $\omega = 0.2 \text{ rad/sec}$ was used.

Fig. 8 Ground-based simulator



One of the results demonstrating the effectiveness of the proposed predictive display in compensating the time delay is shown in fig. 9.

Fig. 9 Effect of the time delay suppression

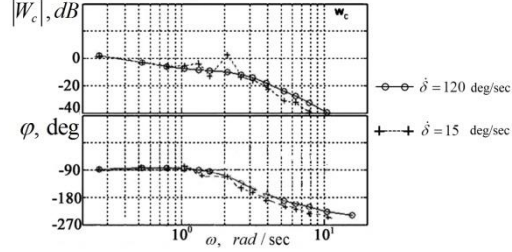


It is seen that the proposed law for the compensation of the time delay provides approximately the same accuracy as in the case when $\tau = 0$.

2.3 The Suppression of the Rate Limit Effects

The effect of the actuator rate limit on the piloting process depends on the aircraft's static stability margin. In case of a statically stable aircraft, the excess of the actuator rate limit causes the deterioration of the equivalent controlled element characteristics: the increase of the phase delay and appearance of the resonant peak in its frequency response (fig. 10).

Fig. 10 The influence of $\dot{\delta}_{\max}$ on the controlled element dynamics (from [11])



As a consequence, the pilot tries to compensate the aircraft delay by generating his lead compensation which deteriorates the closed-loop system characteristics and causes a PIO event (PIO category 1, [4]). For a statically unstable aircraft, the pilot's actions can cause a more serious consequence – the unstable divergent oscillations (PIO event, category 2, [4]) which will lead to a crash of the plane. The development of means of suppressing the rate limit effects in case of a statically unstable aircraft is considered below. The following means were investigated:

- Reconfiguration of the flight control system (FCS) law;
- Use of the predictive display;
- Integration of the reconfigured flight control system and the predictive display.

Reconfiguration of the FCS law was realized by decreasing the feedback gain coefficients for a reduction of the elevator deflection rates $\dot{\delta}$ in case of a sudden decrease in the rate limit $\dot{\delta}_{\max}$. The pitch rate q and the normal acceleration n_z were used as feedback signals to provide the necessary flying qualities for the unstable aircraft dynamics with the short period motion transfer function $W_c = \frac{q}{\delta_e} = \frac{M_\delta(s - Z_\alpha)}{s^2 + 2\xi\omega_{sp}s + \omega_{sp}^2}$, where $\omega_{sp}^2 = -0.29$ rad/sec (fig. 11,

$Z_\alpha = -1.4$ rad/sec). The gain coefficients K_q and K_n (see table 1) were selected to provide the dynamic configurations corresponding to the configurations HP-2.1 and HP-5.1 from the Have PIO data base [12] and characterized by different flying qualities.

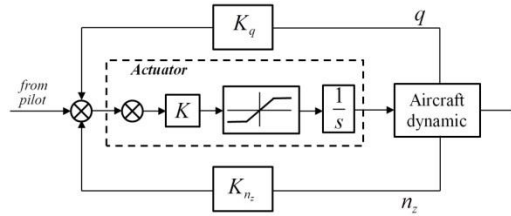
The parameters of the gain coefficients K_q and K_n and average pilot Cooper-Harper opinion ratings PR obtained in flight tests [12] are given in table 1.

Table 1 Gain coefficients and pilot rating's

Configuration	K_q	K_n	PR
HP-2.1	4.14	1.59	2.3
HP-5.1	2.62	1	3.5

The lower values of the coefficients corresponding to the dynamic configuration HP-5.1 leads to lower rates of elevator deflection in comparison with configuration HP-2.1. It might be sufficient in case of the rate limit.

Fig. 11 The flight control system scheme



The other possible means of reducing the elevator deflection rates is the flight path predictive display. In the case when the time delay is zero, the controlled element dynamics, taking into account the display law, are defined by the equation (2). Its phase frequency response characteristics are more than -180 deg in the frequency band $\frac{1}{T_{pr}} < \omega < \omega_{sp}$. It means that such dynamics do not require considerable pilot lead compensation and more rapid actions in comparison to the case when pilot tracks the aircraft altitude.

Using the technique discussed above for determining the T_{opt} it was obtained that $T_{pr}^{opt} = 0.9$ sec for configuration HP-2.1 and $\dot{\delta}_{max} = 60$ deg/sec and $T_{pr} = 1.4$ sec for the configuration HP-5.1 for the same rate limit. The prediction time has to be increased after the hydraulic failure as it causes a decrease in the actuator rate limit. It extends the frequency range where the controlled element phase frequency response is more than -180 deg and allows excluding the active and rapid pilot actions causing a high rate of signals transmitted to the actuator. The mathematical modeling of the linearized pilot-aircraft system showed that the optimum prediction time is equal to 2 sec when the rate limit decreases up to 15 - 30 deg.

The experimental investigations were performed on the same MAI ground-based simulator which was used for investigating the influence of the time delay. The major part of the experiments was carried out when the sudden decrease of the rate limit $\dot{\delta}_{max}$ occurred at 20 sec in the dynamic configuration HP-2.1. The landing task was investigated in the following conditions:

1. Configuration HP-2.1 with the actuator characterizing $\dot{\delta}_{max} = 60$ deg/sec for the whole duration of the experiment;
2. Configuration HP-2.1 with a sudden decrease of the rate limit up to 30 deg/sec;
3. Configuration HP-2.1 with a sudden decrease of the rate limit up to 30 deg/sec and a simultaneous increase of the prediction time T_{pr} in the predictive angle law;

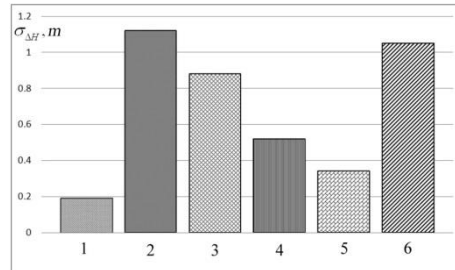
4. Configuration HP-2.1 with a sudden decrease of the rate limit up to 30 deg/sec and a simultaneous decrease of feedback coefficients up to the values providing the dynamic configuration HP-5.1;
5. Configuration HP-2.1 with a sudden decrease of the rate limit up to 30 deg/sec and a simultaneous decrease of the feedback coefficients up to the values providing the dynamic configuration HP-5.1 and the increase of T_{pr} up to 2 sec;
6. Configuration HP-2.1 with a sudden decrease of the rate limit up to 15 deg/sec and simultaneous decrease of the feedback coefficients up to the values corresponding to the values providing the configuration HP-5.1 and the increase of T_{pr} up to 2 sec.

Three operators participated in the experiments, whose qualification was discussed in section 2b. More than 100 experiments were carried out by means of ground-based simulation.

The accuracy of the tracking was evaluated by the variance of error $\sigma_{\Delta H}^2 = \frac{\sum (h(t) - H_i)^2}{N - 1}$ where H_i is the program trajectory (glide path), $h(t)$ – the aircraft altitude.

Results of experiments given in fig. 12 demonstrates that the reduction of the rate limit up to 30 deg/sec leads to a considerable deterioration of accuracy of the path tracking (case 2).

Fig. 12 The effectiveness of different means



The mean square error $\sigma_{\Delta H}$ in case of the dynamic configuration HP-2.1 increases from 0.19 m up to 1.12 m. The increase of the prediction time from 0.8 up to 1.4 sec allowed the improvement of the accuracy up to 1.4 times ($\sigma_{\Delta H} = 0.88$ m, case 3) and the change in the feedback coefficients, led to the transformation of the linear dynamics from HP-2.1 to HP-5.1, which caused the decrease of $\sigma_{\Delta H}$ up to 0.52 m (case 4). The simultaneous reconfiguration of the predictive display law and the feedback gain coefficients led to the improvement of the accuracy up to 34% more in comparison to the previous case (case 5).

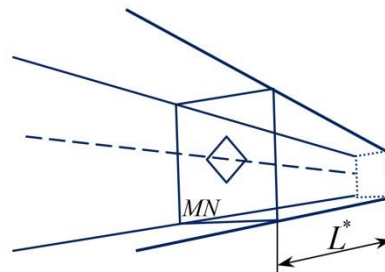
The experiments demonstrated that in the case of a sudden reduction of the rate limit up to 15 deg/sec the tracking task cannot be carried out without a sim-

ultaneous reconfiguration of the display law and the flight control system gain coefficients. In case 6, the error was rather high ($\sigma_{\Delta H} = 1.05 \text{ m}$) but in general, the tracking of the glide slope was a stable process. Thus the simultaneous change of the gain coefficients and the prediction time allowed to decrease the error of the program trajectory tracking and to provide the stable control process even for the case when the rate limit decreases 4 times.

4 The Influence of the Preview of the Planned Trajectory

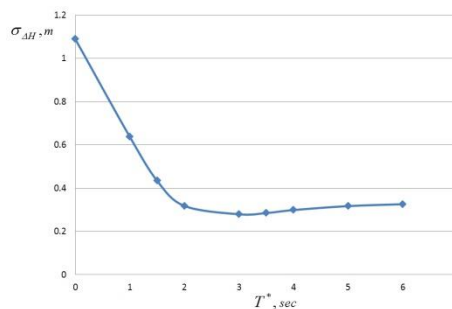
The experiments analyzed above were carried out in conditions when the displayed corridor has a rather long length L^* behind the surface MN (fig. 13).

Fig. 13 Display with preview information



The demonstration of this part of the corridor allows pilot to carry out the tracking with preview of the planned trajectory. Due to this, a separate set of experiments was carried out to expose the rational value of $L^* = \frac{T^*}{V}$ (T^* is the preview time, V is the aircraft velocity). The mean square error $\sigma_{\Delta H}$ measured for the different preview time are given on fig. 14.

Fig. 14 The effect of the preview



It is seen that the preview time has to be limited by the values of $T^* = 2 \div 3 \text{ sec}$. The similar character of the function $\sigma_e = f(T^*)$ was obtained

in [8]. However the optimal values of $\sigma_{\Delta H}$ here are smaller ($T^* = 0.4 \div 0.6$ sec) which can be explained by the different controlled element dynamics ($W_c = \frac{\varepsilon_{pr}}{\delta_e} = \frac{K_c}{s}$), and the forcing function investigated there.

In [8] the recommended value T^* was obtained as the result of definition of the dependence $\sigma_e^2 = f(L)$, where $e = i - y$ and y is the output controlled element dynamics (in our case $y = \varepsilon_{pr}$). In the considered paper $e = H - H(t)$, where $H(t)$ is the current aircraft altitude, $H^*(t)$ – the current altitude of glide.

Thus, in addition to the prediction time T_{pr} , the preview time is the major variable which has to be defined in predictive display design.

Conclusion

The developed technique for the predictive flight path display design takes into account the time delay in aircraft dynamics. The ground-based simulation demonstrates that the revised predictive law allows to suppress the effect of the time delay. It was shown that the sudden decrease of the rate limit requires the reduction of the gain coefficients and prediction time constant T_{pr} in equation for the predictive path angle. The simultaneous change of these parameters provided the stable flight even for the fourfold decrease of the rate limit. The potential of the pilot to realize the tracking with preview when the 3D tunnel is displayed behind the surface moving inside the corridor was shown. Integration of the predictive display with the image of preview planned trajectory allows to considerably improve tracking accuracy. The experiments disclosed the existence of the optimal preview time close to 2 - 3 sec.

Acknowledgments

The results included in the paper are the results of the investigation which were sponsored by the Ministry of Education and Science (contract № 9.7465.2017/8.9).

References

1. D. McRuer, D. Johnston, "Flying qualities and control system characteristics for superaugmented aircraft", STI-TR-1202-1, September 1984

2. R. Hoh, T. Myers, I. Ashkenas, R. Ringland, S. Craig, "Development of handling qualities criteria for aircraft with independent control of six degrees of freedom", AFWAL-TR-80, Jan. 1981
3. D. McRuer, D. Graham, "A flight control system century: Triumphs of system approach", *Journal of Guidance, Control and Dynamics*, Vol. 23, № 2, 2003, 161-173 pp.
4. D. McRuer et al., "Aviation safety and pilot control", National Press, Washington D.C., 1997
5. A.V. Efremov, A.V. Ogloblin, "Development and application of the methods for pilot-aircraft system research to the manual control tasks of modern vehicles", AGARD Conference Proceedings, AGARD-CP-556.
6. A.V. Efremov et al, "Pilot as a dynamic system", *Mashinostroenie*, 1992
7. A.V. Efremov et al, "Flying qualities improvement for the vehicles with time delay in their dynamics", 30th Congress ICAS, Korea, 2016
8. L. Reid, N. Drewell, "A pilot for tracking with preview", NASA-University, Eight annual conference on manual control, 1972
9. G. Sachs, "Perspective predictor flight – path display and minimum pilot compensation", *Journal "Guidance, control and dynamics"*, Vol. 23, №3, May-June, 2000
10. A.V. Efremov, M.S. Tyaglik, "The development of perspective displays for highly precise tracking tasks", In the book "Advances in Aerospace Guidance, Navigation and Control", Springer, Germany, 2011
11. A.V. Efremov et al, "Investigation of pilot induced oscillation tendency and prediction criteria development", Report WL-TR-96-3109, May 1996, Wright Lab USAF
12. E. Bjorkman, "Flight test evaluation of techniques to predict longitudinal pilot-induced oscillations", Ph.D. Thesis, 1996